ISSN: 2521-2915 (Print)
ISSN: 2521-2923 (Online) Pakistan Journal of Geology (PJG) 2021, VOLUME 5, ISSUE 2

# Delineating and Interpreting the Gold Veins Within Bida and Zungeru Area, Niger State Nigeria, Using Aeromagnetic and Radiometric Data

**Aliyu, Shakirat Bukola[a], Adetona, Abbass. Adebayo[a], Rafiu Abdulwaheed Adewuyi[a], Ejepu Jude[a], Adewumi, Taiwo[b*]**

[a]Department of Geophysics, School of Physical Science, Federal University of Technology Minna.
[b]Department of Physics, Faculty of Science, Federal University, Lafia, Nigeria
*Corresponding author: tydon4real@yahoo.co.uk, taiwo.adewumi@science.fulafia.edu.ng

***DOI: 10.2478/pjg-2021-0006***

**Abstract:**
Both Airborne Magnetic and Radiometric datasets were employed to interpret the geology and geological structures that serve as host to gold and associated minerals within the Bida and Zungeru, Niger State, Nigeria. An area of 55 by 110km$^2$, contained within the cretaceous sediments of Bida Basin and the meta-sediments of Zungeru-sarkin-pawa schist belt. Data interpretation involve the application of a mathematical algorithm for data enhancing such as, Reduce to the Equator, Analytical signal, First Vertical Derivative, and Centre for Exploration Targeting (CET) to the magnetic data, and Ternary imaging to the radiometric data, with a sole aim of mapping geological structures such as faults fracture folds joints and geological boundaries and possible gold mineralization veins that arise from hydrothermally altered zones. Two major geological units inhibit the study area, the cretaceous sediment, and the meta-sediments, major feature identifies within the Cretaceous sediment are the folds majority of which are located within the contacts. The result of the 1VD display is the vivid picture of the observed structural features such as faults fractures folds' contacts labeled F1 to F8 both within the high region of magnetic susceptibility (in red) and low regions (in blue) geology contacts (yellow), folds (bold yellow) all across the field. Prominently at the North-Western corner of the study area are sets of linear structure that trend NE-SW, located within the contacts between the mylonites and the amphibolites and the belt-type meta-sediments located around Katakwo, Gindei, Kwange, Gabas and Akusu villages. Equallyworth mentioning are sets of lineament (in blue) trend E-W all across the mid-region of the study area, precisely at the Eastern corner within and below the Federal University of Technology Minna around Kata-eregi, Sabon-Dagan, Kakaki down Minkwoigi, Sunbwagi, Kakagi, Sabon dagga, and Bobo-shiri towns, where the majority of volcanic activities must have been recorded. The airborne radiometric show mobilization of the immobile thorium Th, concentration, and this also indicated hydrothermally altered zones. The increase in potassium concentration and decrease in K/Th relation observed from radiometric interpretation are very pinpointing of hydrothermal activities within the study area. The gold mineralisations are found within this vein and in the adjacent, highly deformed host rock located below the Federal University of Technology Minna Campus. The deformation seems to comprise principally of pebbly schist, amphibolites along fine-grained and magnetite.

**Keywords:** Airborne; Hydrothermal altered; Centre for Exploration Targeting (CET); First Vertical Derivative (1VD.)

## 1.0. Introduction:

Various geophysical methods have been employed in the exploration of solid minerals such as gold, techniques such as seismic, gravity, magnetic and electrical are among the most commonly used [1-3]. Each of these methods employs the specific characteristics of the mineral in question to delineate its deposits. The ambiguities that arise from each of such manner leaves no one in doubt about their limitations. In gold exploration, the choice of density as a unique ability is limited by the quantity of gold in the host rock making any significant contribution to the overall density. A similar situation arises when the conductivity of gold prompts the choice of electrical method. Outside the fact that other factors such as the presence of water can enhance conductivity, the quantity available may not significantly affect the overall conductivity of the host. Therefore, an integrated method coupled with the good geological background can help reduce the number of ambiguities. Integration of Magnetic with Gravity and Resistivity has yielded promising results in regions where mineralisation is structurally controlled [4-6]. It was noticed that the magnetic and radiometric regions where the structural veins coincide with regions of alterations in rocks are associated with Uranium and real-metal mineralisation zones [7,8].

Exploration for gold within Minna, Zungeru, Kafin-tela and Sarkin Pawa axis can be dated the back the to late 1940s when veterans from the Second World War migrated to these regions. A careful study shows that most of these explorations by these" unskilled miners" were within the lithological contact, shear and fractured zones around the schist belts. However, most of these explorations resulted in low yields due to lack of proper geophysical studies and inadequate tools. The present research is taking a careful look at delineating these subsurface structures from aeromagnetic data and correlating them with an area of hydrothermal alterations to provide a database consisting of precise coordinates and depth to these deposits for better gold exploration within the region. Both within the old western granite and the central old and young granite of Nigeria, the regional NE-SW to N-S fault and shear zones are regions where these mineral veins are confirmed. These veins often inhibit the general N-S to NNE-SSW structural grain on the basement signifying different geological settings and an indication of several periods of mineralisation.

This project aims to delineate the geological structures such as lineaments, faults, dykes, folds, and other intrusive bodies that could be the host for gold mineralisation using aeromagnetic and radiometric data. Two fundamental factors motivated this research work. These are:

1. It has been observed that numerous unregistered" artisanal miners" are scattered across Niger state including part of the study area (Bida Zungeru axis). Who employed their trial-and-error methods that generally results in massive wastage of the required minerals?

2. The decision by the management of the Federal University of Technology Minna, (whose campus is located between the Bida and Zungeru data sheet) to go into gold exploration to improve its internally generated revenue. Thus, a detailed geological analysis of this field is required to determine the exact location and depth to these structures.

### 1.1. Location of the Study Area

The study area is located within the Bida (184) and Zungeru (163) sheets, bounded by the longitude 6°00'E and 6°00'E and latitude of 9°00'N and 10°00'N as show in figure 1 below. It occupies an area of 110 km by 55 km starting from Bida sedimentary basin extending into the Zungeru meta-sediments.

### 1.2. Geology of the Study Area

Gneisses, migmatites, and associated Meta-sedimentary rocks of the Nigerian basement are usually called the gneissic complex or the migmatite-gneiss complex. Truswell and Cope classified the metamorphic rocks of the Kusheriki sheet into three formations: The Kusheriki Psammite, the Birnin Gwari Schist, and the Kushaka Schist Formations (Truswell and Cope, 1963). Metamorphic and igneous rocks of Precambrian to early Palaeozoic age are exposed in about 50% of the area of the study area in the northern and south-eastern parts of the sites. Upper cretaceous underlies south southern and north-western part of the area to recent sedimentary rocks of the Bida Basin which account for the remaining 50% of the surface geology of the sheet. The crystalline rocks include migmatites, gneisses of varying composition and texture; Mylonitic rocks (the Zungeru Mylonites); meta-sedimentary rocks including amphibolites, schist, talc actinolite, and talc chlorite schist, interlayer with the gneissic complex; low-grade schist which occupy N-S trending belts, and rocks of the Older Granite suite which intruded the metamorphic rocks. Two generations of migmatites were distinguished an early migmatite and a late migmatite series. The early migmatites are believed to have been formed during the early history of the basement, before the deposition of the rocks of the schist belts. The late migmatites, after referred to as the Pan-African Migmatites, are believed to relate to the emplacement of the Older Granites. Low- to medium-grade meta-sedimentary, the Ushama, the Birnin Gwari, and the Kushaka belt in the northern.

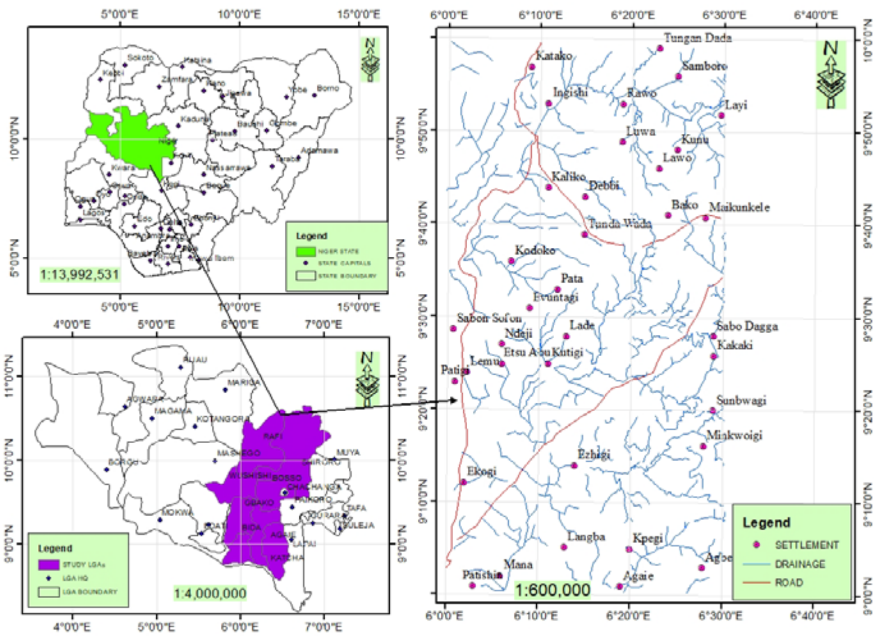


**Figure 1.** Location Map of the Study area.

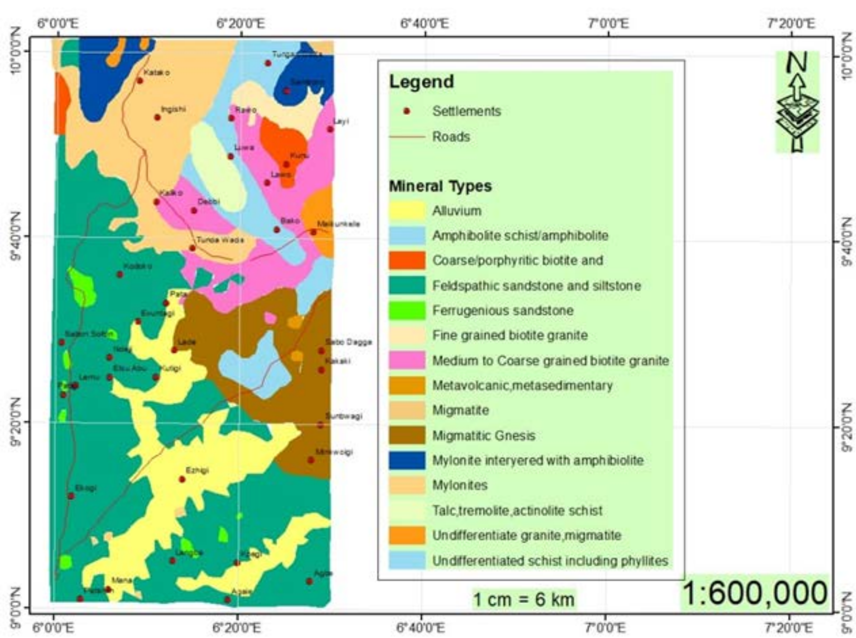


**Figure 2.** Geology Map of the study area

Half of the sheet (Rahaman, 1988). Relics of schist arc very common within the granitic rocks. The most extensive of these occurs in and around the River Chanchaga, along the Minna-Bida road, far from the prominent outcrops of the schists. Small-scale structures in the schist formations indicate four phases of deformation. The initial folding of the rocks of the schist belts during the first episode of deformation ($D_1$) was accompanied by extensive deformation of parts of the early gneissic complex and by the formation of the Zungeru Mylonites. The schist belts and the Zungeru Mylonites were deformed together during subsequent movements ($D_2$-$D_4$) and they now have parallel structures. The unconformity between the underlying basement and the adjacent Birnin Gwari Formation is believed to have been obliterated during the $D_1$ deformation. The metamorphic rocks were later invaded by the widespread Older Granites. Field relations show that there are at least three major episodes of igneous intrusion in the region. The first episode led to the emplacement of medium to coarse-grained granites. In this episode, the Kushaka Schist formation was extensively migmatised by migmatitic injection to form the Pan-African Migmatites. These were followed by the intrusion of coarse-grained biotite granites which also include the leucosome to the schistose paleosome in the Pan-African Migmatites. The last significant plutonic activity led to the emplacement of very coarse-grained to coarsely porphyritic granite which forms elongate or oval-shaped bodies cutting the earlier phases of intrusion as well as the metamorphic rocks (Ajibade et al., 2008). Whole-rock Rb/Sr age determination on the Zungeru Mylonites, the Birnin Gwari, and the Kushaka Schist Formations and some of the Older Granites yielded ages of 500 - 700 My which all pegmatitic material. The other type, the Pan-African Migmatites, in general, have simple structures that include alternating schistose, granitic, or pegmatitic layers.

## 2.0. Theory of method Methods

The composite maps will be producing using Oasis Montaj, ArcGIS, and the Golden Software (Surfer 11). The theories of digital analytical tools are given in sections 4.1 to 4.5.

### 2.1. Vertical Derivative

In an attempt to attenuate the long wavelength regional features within a potential data and in the same vein, we accentuate the shallow features that are high in frequency of occurrence and this makes the vertical derivative comes in bandy.
The function can be mathematically related as

$$L(r) = r^n \tag{1}$$

where n depicts the order of differentiation generally 1 or 2,' r' signifies the wavenumber in radians per ground unit observe that r=2pl, where L is cycle/ground unit in which the survey was conducted e.g. metres, feet, kilometre etc.

### 2.2. Analytical Signal

Magnetic data most significantly, within the equator exhibits high dipolar signatures, in which both the positive and negative susceptibility exhibit peaks. The derivative analytical signal removes effects of angle inclination and declination from the magnetic data. Thereby, giving the anomaly the required symmetry and placing the anomaly directly above the causative body. The 3-D analytical signal at a location (x,y) can be obtained from three orthogonal gradients of total the magnetic field using the expression.

$$\left|A(X,Y)\right| = \sqrt{\left(\frac{dT}{dx}\right)^2 + \left(\frac{dT}{dY}\right)^2 + \left(\frac{dT}{dZ}\right)^2} \tag{2}$$

Where |A(x,y)| is the amplitude of the analytic signal

T is the value of the magnetic field at (x,y)

dx is the horizontal derivative over a 2D magnetic contact at (x ε 0) and at depth h can be defined by the expression

$$\left|A(X)\right| = \alpha \frac{1}{\left[h^2 + x^2\right]^{\frac{1}{2}}} \tag{3}$$

Where α represent the amplitude factor
$\alpha$= 2Msind (I-cos$^2$ (I) sin2 (A)
h signifies the depth to the top of the contact
M is the strength of magnetisation
d is the dip of the contact
I is the inclination of the magnetisation vector
A is the magnetisation vector direction
The equation above explained the analytic signal for a simple bell-shaped function.
Note that: the peaks amplitude is directly proportional to the magnetisation at the edge as defined by the equation above.

### 2.3. Euler depth determination method

The need to determine the depth to the major structures delineated prompt for the use of Euler's deconvolution algorithm. The knowledge of these depths will aid in the ease of exploration of available minerals. Euler's depth has a special advantage over other depth estimation method; it targets the centre to the anomaly of interest rather than depth of overburden of the field and it employs the structural index for each of the anomaly targeted, equally its degree of accuracy can be improved by filtering its results.

A formulation of Euler's homogeneity relationship given by a group researcher shows that [11]:

$$\left(x-x_0\right)\frac{\delta T}{\delta X}+\left(y-y_0\right)\frac{\delta T}{\delta Y}+\left(z-z_0\right)\frac{\delta T}{\delta z}=N\left(B-T\right) \tag{4}$$

Where *($x_o$, $y_o$,* and *$z_o$)* are the magnetic source positions whose entire magnetic intensity field T is ascertained at *(x, y, z).* The total field with a regional value of B. N represents a structural index which is equal to three for a point dipole and two for a vertical pipe. An index of one shows up to work for dyke and contacts. A group researcher automated the solution of this linear equation for gridded data to generate solutions for the positions and depths of magnetic sources [11].

### 2.4. The Centre for Exploration Targeting (CET) Grid Analysis Plug-In for Structures

Centre for exploration targeting a grid analysis plug on for structural analysis automatically delineate peak linear structure within extensive potential data. It consists of five separate stages which are.

By employing standard deviation σ of a cell values $x_i$ given by

$$\sigma=\sqrt{\frac{1}{N}\sum_{i=1}^{N}\left(x_{i\,-\,\mu}\right)^2} \tag{5}$$

The gridded data is

1) Separated into two sections as,
    a. Regions where data values within the local neighbourhood show little variation.
    b. Area where the data indicate high variation within the neighbourhood.
2) The region of high variations are given phase symmetry by using the natural frequency based approach
3) This followed amplitude threshold where the maximum values where preserved and the minimum where attenuated using non-maximal suppress
4) Lastly skeleton to vector was applied were the variation of the magnetic field values was vectorised in the direction of maximum are then lineated for mapping.
5) Centre for Exploration Targeting (CET) has two main advantages over vertical derivative and generalised derivative which are
    a. CET being an automatic method even small lineament in a large area that may escape visual observation cannot flee in CET
    b. The coordinate for each of the delineated structures are automatically safe into a database on UTM format by Geosoft inc and can be extracted from the software into any other form.

## 3.0. Materials and Methods

### 3.1. Source of Data

The data used for this analysis were obtained from the Nigerian Geological Survey Agency (NGSA) in a digital/grid format. A high- resolution Airborne Geophysical Surveys required are magnetic, radiometric, and limited electromagnetic surveys which purposed are to assist and promote mineral exploration, carried-out in Nigeria between 2003 and 2009. The surveys for the two phases were carried out from 2004 to 2009. Fugro Airborne Survey Limited, Johannesburg achieved this by carried out the flying for data collection in all projects.

Technical details involve:

Flight Parameters;

| | |
|---|---|
| Total line kilometres: | 36,500km (Ogun state), 1,930,174 km (Phases I & II) |
| Flight line spacing: | 500 metres |
| Terrain clearance: | 100 m (Ogun state), 80 m (Phases I & II) |
| The direction of Flight: | NW – SE |
| Lines spacing: | 2 km |
| Lines direction: | NE – SW |
| Measured Parameters: | Magnetic gradient and Multi-channel radiometric |

### 3.2. Methods

The data collected at the Nigerian Geological Survey Agency (NGSA), was subjected to the following corrections:

Magnetic Compensation
Noise Removal
Diurnal Removal
Micro levelling
IGRF removal of 33,000nT.

The IGRF reduced aeromagnetic data and aero-radiometric of Bida and Zugngeru sheets, both in gridded format was obtained from the Nigeria Geology Survey Agency. A geology map of the area interpreted. A good speed personal computer with installed Oasis Montaj 9.2 edition ArcGis 10.3 edition and Surfer13, are essential to carry out a significant analysis. The objectives of this study are to:

i. Compute and interpreted the Total Magnetic Intensity (TMI) of the area to show regions of high and low magnetic susceptibility

ii. Compute the analytical signal to place anomalies directly above the causative body.

iii. Obtain the horizontal derivative, vertical derivative and Central Exploration Targeting (CET) to delineate structures that could be faults, fractures, intrusive bodies, and lineaments that are vein.

iv. Apply the Euler Deconvolution method to the dataset to get depth to the magnetic source.

v. Produce the concentration maps for potassium, thorium, and uranium of Bida (Sheet 163) Zungeru (Sheet 184) to delineating regions of highs and lows for the three elements

vi. Produce ternary map by combining the data of Potassium K (in red), Thorium Th (in green) and Uranium U (in blue) to map geology contact and correlate with Geology map

vii. Delineate regions of hydrothermal alterations within the study area

viii. Correlate the structure obtained from the total magnetic field with areas of hydrothermal alterations from radiometry analysis.

## 4.0. Result and Interpretation

### 4.1. Total Magnetic Intensity (TMI) Map Production

The gridded aeromagnetic data obtained from NGSA whose parameters were stated above were gridded using minimum curvature mode on the Oasis Montaj and display in the colour aggregate map (Figure 3). The chart exhibits the variation in magnetic susceptibility that forms the lithology within the area. Being an area that is close to the equator the effect of the earth's field plays a significant role in the variation of susceptibility; areas with high magnetic susceptibility are showing lows magnetic values while regions with less magnetic value depict high magnetic susceptibility. Magnetic values within the area range from -119 nT to 147.9 nT. The lower end of the southern part shows relatively low vulnerability these can be attributed to the degree of sedimentation within the terminal point of Bida Basin, clusters of highs, and lows dominant the remaining part of the field. The eastern end depicts pronounced activity due to the rapid variations in field susceptibility within close distances.

### 4.2. Total Magnetic Intensity (TMI) - Reduce to Equator (RTE)

The TMI-RTE was computed and mapped, this helps in archiving the symmetry for the anomaly that exhibits dipolar nature due to the non-vertical inducing field, (Figure 3) depicts both positive and negative anomalies coming from magnetic rocks within the region. The meta-sediments at the mid-eastern part of the area show appreciable high susceptibility this is generally due to intrusive activities of undifferentiated granite. The belt type schist and mylonites also show some much susceptibility.

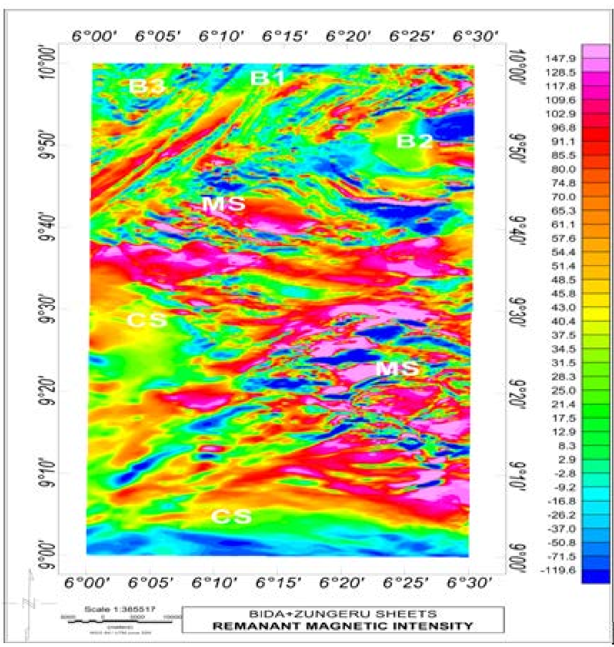


**Figure 3.** Total Magnetic Intensity Map with 33000nT removed as IGRF.

### 4.3. Result of Analytical Signal

The analytical signal map was carefully computed to attenuate sources showing negative susceptibility for more precise interpretation. The 3D analytical signal requires the horizontal derivatives in x, y, and z but the z part was achieved in the frequency domain after the Fourier transform. Analytical signal helps remove the dependence of the residual field on the angles of declination and inclination, thereby positioning the anomaly directly above the causative body. The resulting Figure 4 shows the regions of meta-sediments having a high amplitude signal, a clear indication that the amplitude signal is a reflection of magnetisation of the causative body [12,13]. A clear demarcation is observed between the cretaceous sediment at the lower part and regions of meta-sediments that has undergone several degrees of deformation. The weak magnetic susceptibility values within the meta-sediments depict intrusive felsic formations such as B2 and MS. In contrast, strong magnetic susceptibility within the same meta-sediments is regions of mafic intrusive bodies such as MS, and B3. Significant linear structures at the Eastern corner of the area are lineaments at the contact between different geological formations.

### 4.4. Result of First Vertical Derivative

The first vertical derivative models help in attenuating the long-wavelength magnetic anomaly within the field and this is important in improving closely spaced resolution and superimposed anomalies. Thus to avoid a noisy result an appropriate upward continuation of 100 meters was applied to the TMI-RTP before carrying out the 1VD. The development of the 1VD in Figure (5) display are a vivid picture of observed structural features such as faults fractures folds' contacts F1-F8 both within the high regions of magnetic susceptibility (in red) and low areas (in blue) geology contacts (yellow), folds (bold yellow) all across the field. Prominently at the North-Western corner of the study area are sets of linear structure that trend NE-SW, located within the contacts between the mylonites and the amphibolites and the belt-type meta-sediments. Equallyworth mentioning are sets of lineament (in blue) trend E-W all across the mid-region of the study area. Precisely at the Eastern corner within and bellow the Federal University of Technology Minna around Kata-eregi, Sabon-dagan, Kakaki down to Kutirko, where the majority of volcanic activities must have been recorded. A prominent feature unavoidable is the spherically shaped intrusive bodies at the upper part of the study area marked by B1 and B2 interestingly these intrusive bodies shows relatively low susceptibility on the Analytical signal map. All the folds delineate are located and the edge/contact between the Cretaceous sedimentary formation and the meta-sediment basement region.

### 4.5. Result of Euler Deconvolution

Euler Deconvolution is a depth estimation method that takes advantage of the structural index on either a vertical pipe, dyke contact within a complex geological formation index value such as 0, 1, and 2 are assigned for bodies like contact, Dyke, and pipe respectively. In this structural analysis index of 0, 1, 2 were combined and the resulting filter to accommodate the objectives delineating structures that are host to gold and other associative minerals such as silver. Results from the analysis figure 6, show that majority of these structures are situated between 30 to 300meters all across the field within the meta-sediment. Generally, depth estimates within 30 to 160 meters dominate the field most especially around Sabon-dagan, Kakaki, Sunbwagi, Minkwegi, and Kapagi.

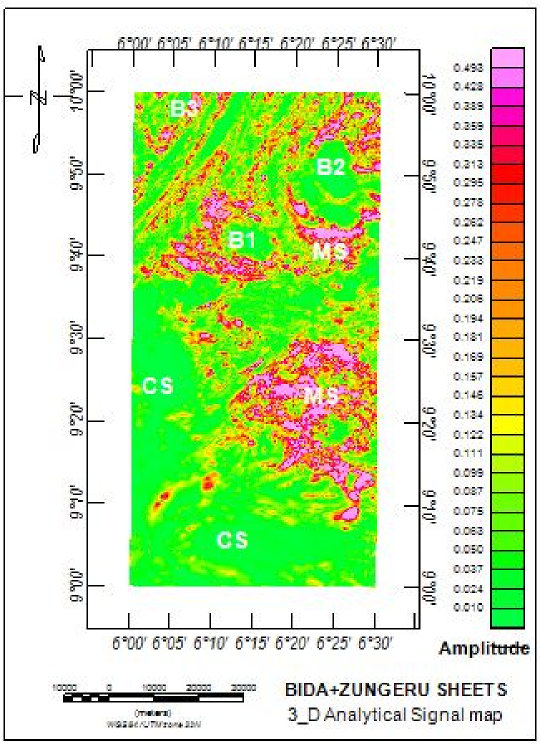


**Figure 4.** Analytical Signal Map

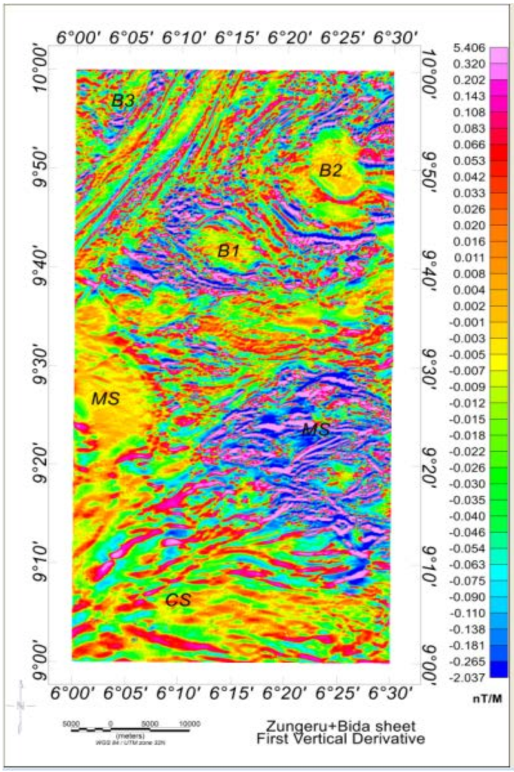


**Figure 5a.** First Vertical Derivatives

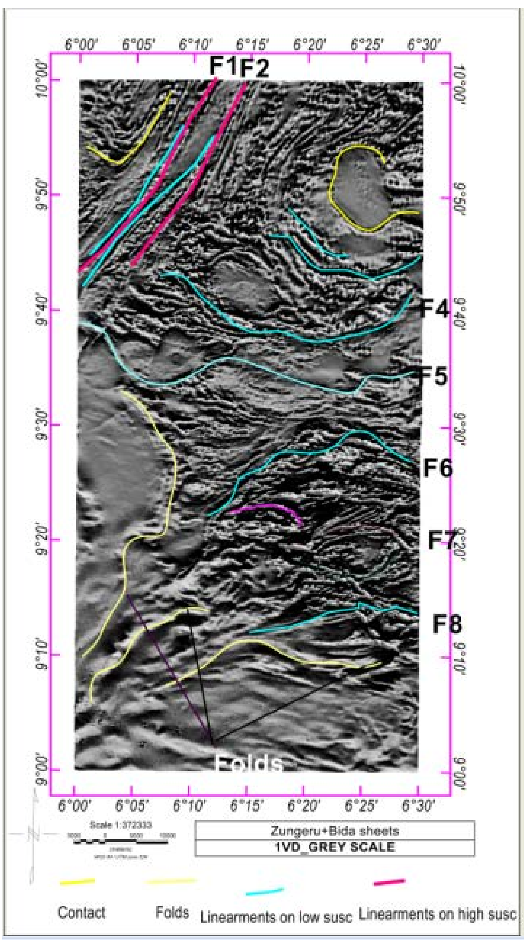


**Figure 5b.** First Vertical Derivative in greyscale with delineated structure

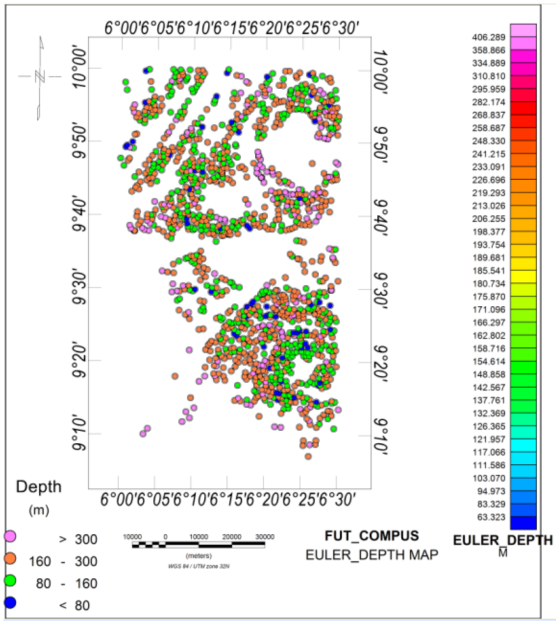


**Figure 6.** Euler Deconvolution Depth map

**4.6. Result of Centres for Exploration Targeting (CET)**

Centre exploration targeting is an automation method of delineating lineaments. The results from CET interestingly correlate the lineaments mapped on the 1VD though more detail than that what was observed on the first vertical derivative. An added advantage is that the Centre exploration targeting was able to extract the coordinates where these lineaments were observed. Coordinate of these significant structures and lineaments that shows the degree of mineralisation has been mapped on figure 4.6 most interestingly is between longitudes 6˚20E to 6˚30Eand latitude 9˚10N to 9˚30N.

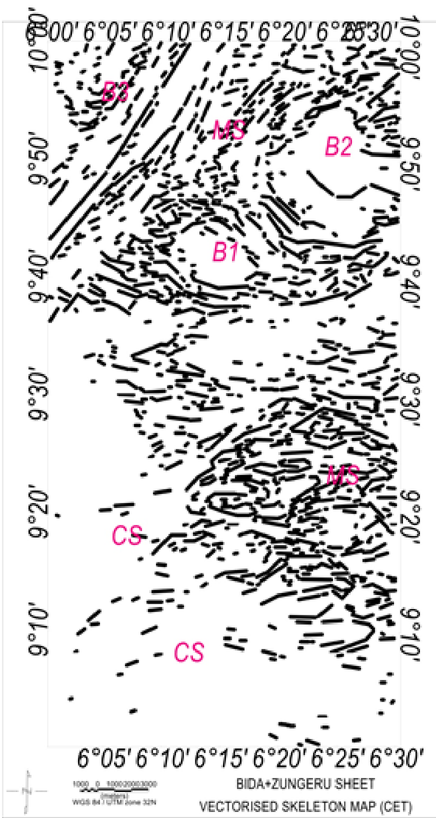


**Figure 7.** CET Structural map with relevant coordinates

**4.7. Result and Interpretation of Radiometric Data**

Representing Uranium, thorium, and potassium with blue, green, and red colouration respectively, the ternary map was produced to represent an individual concentration of the gamma radiation and corresponds to slight variations in their relative amount. The map shows a sharp contrast between the geological formations identifies within the study area. The regions containing the amphibolites, mylonite, and migmatite shows darker than the neighbouring shapes indicating weak content in potassium, thorium, and Uranium. The white area in the composite map is an indication of vital content in K, Th, and U. At the same time, yellow indicates site of strong potassium and thorium but weak Uranium content. The magenta shows an area of strong potassium and thorium but low Uranium. Blues and dark blue regions marked the study areas most of which are within the contact and fault regions, they are related to the belt type granite also at the eastern corner between 9°15- 9°30N and below the spherical bodies B1, B2 equally within B3 and MV indicating the low intensity of potassium and thorium (Figure 8) but high Uranium. The high Uranium within these regions suggests young granitoid intrusions accompanied by low magnetic intensity. Below the FUT Minna region excessive weathering must have used up most of the uranium content this informs the magenta colouration observes just below latitude 9°30N (Minkwoigi, Sunbwagi, Sabon dagga, and Bobo-Shiri). It was followed by Hoover and Pierce that airborne gamma-ray surveying marks of deposit of gold were chargeable with potassium being the most dependable guide regions hosting gold within quartz vein, hydrothermal alteration of the causative body can provide reliable links [14]. In this research potassium is related to most favourable host rocks. Low potassium anomalies are observed along with the contacts between the cretaceous sediments and the meta-sediments trending NW-SE and within the mylonite at the north-western corner of the study area. Hydrothermal zone, faults, veins, and foliation host mineralisation of gold within the study area. The contact zone depicts low potassium and high thorium and Uranium (figure 4.10) respectively. The weak potassium anomaly could show potassic alteration associated with an increase in the fluid entry that migrates through low pressure and high faulted zones within this area [15].

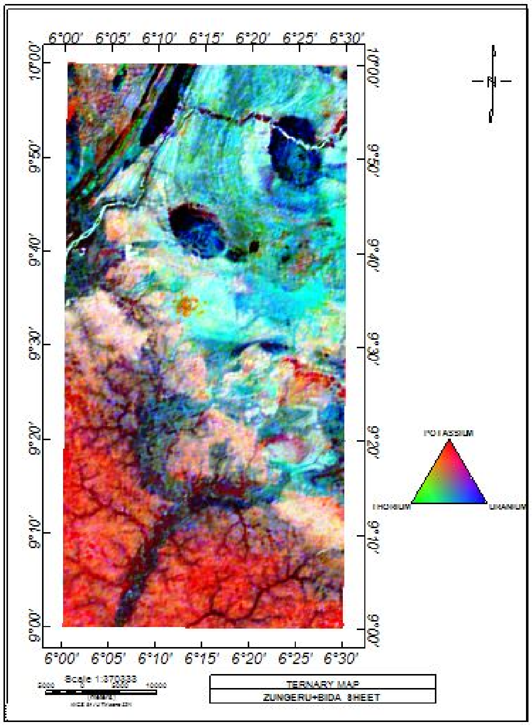


**Figure 8.** Ternary map from a combination of Potassium, Thorium, and Uranium concentrations.

## 5.0. Discussion of Results

A distinctive variation observed between cretaceous sediment and the meta-sediments were observed both on the first vertical derivative map on figure 5a, 5b, and the radiometric map figure 8. However, the intrusions within the belt type granite and schist have altered the chemical composition of the majority of the rocks within the study area, which can be seen on both the radiometric concentration distribution and magnetic susceptibility variations. The various changes in concentration of potassium and thorium within primarily the meta-sediments in regions of MV B1,B2 ,B3, and below FUT Minna campus are clear evidence of hydrothermal alterations as observed by mafic volcanic rocks generally lack potassium bearing minerals and K enrichment is not accompanied by Th during hydrothermal alterations [16]. In the magnetic analysis such as the analytical signal, the first vertical derivative revealed contact between meta-sediment and sedimentary formation are demarcated by shear zones, faults, fractures, and low magnetic susceptibility (Figure 5a and 5b). These are due to volcanic activities accompanied by rock deformation and metamorphism especially within the brittle shear zones [16]. The regions that are hydrothermally altered are possible targets that control gold mineralisation of the study area-specific regions delineated and mapped include F1- F6. Below B2 they are strategically located within the mylonite and schist deposit at the NW corner of the area below B2 and B1 within the meta-sediment (MS) below FUT Minna campus around Kata-eregi, Gada, etc within the migmatite at the lower eastern end.

## 6.0. Conclusion and Recommendations

The examinations of the geophysical datasets in the study area provide detailed information into the structural construction. Two central geological units inhibit the study area cretaceous sediment and meta-sediments, major feature show within the Cretaceous deposits are the folds majority are located within their contacts. The mineralisation of gold is strongly characterised by quartz stockwork rocks sourced predominately in granite. The gold can be found within this vein and in the adjacent, highly deformed host rock located around Minkwoigi, Sunbwagi, Kakagi, Sabon Dagga, and Bobo-shiri towns. The deformation seems to comprise principally of pebbly schist, amphibolites along fine-grained and magnetite. It happens in very fine grains, strongly characterised with pyrite and seemed to have been introduced along with carbonate and sulphur which post-date the previous deformation (silica, sericite and iron oxides) [16]. The airborne radiometric showed mobilisation of the immobile thorium (Th) concentration and this also indicated hydrothermally altered zones. The increase in potassium concentration and decrease in K/Th relation observed from radiometric interpretation are very pinpointing of hydrothermal activities within the study area. This reveals major structural features located just below FUT Minna campus around Minkwoigi, Sunbwagi, Kakagi, Sabon dagga, and Bobo shiritown that include shear zone, faults, shear and fault intersections, and fractures systems magnetic anomalies that mainly trend E-Wand NW-SE direction. This maybe attributes to the hydrothermal activity where hydrothermal fluids move to low pressured regions where these faults occur and generate heat destroys the magnetisation within the causative rocks hence low magnetic intensities are related to the delineated faults. The K/Th map also reveals this area with low potassium concentration but high thorium concentration.

### 7.0. Recommendations

From the foreseen results an appropriate ground touting using an electrical or gravity method is recommended at those locations delineated, taking the coordinates into reference, this will validate these results and quantify the reserves.

### 8.0. Appreciations

A profound appreciates to the management of Nigerian Geological agency for making the Aeromagnetic and Aero-radiometric data available and Geosoft inc for the use of Oasis Montaj.

### 9.0. References

[1] C.A. Moreira, S.M. Lopes, C. Schweig and A.R. Seixas, “Geoelectrical prospection of disseminated sulfide mineral occurrences in Camaqua˜ sedimentary basin, Rio Grande Sul State,Brazil”, *Revista Brasileira de Geofı’sica,* Vol. 30, No. 2, Pp. 169–179, 2012.

[2] R.J. Irvine and M.J. Smith, “Geophysical exploration for Epitermal deposits”, *J. Geochem. Explor*., Vol. 36, Pp. 375–412, 1990.

[3] A.F. White, T.D. Bullen, M.S. Schulz, A.E. Blum, T.G. Huntington, and N.E. Peters, “Differential rates of feldspar weathering in granitic regoliths. Geochim. Cosmochim”, *Acta,* Vol. 65, Pp. 847–869, 2001.

[4] W.K. Mohanty, A. Mandal, S.P. Sharma, S. Gupta, and S. Misra, “Integrated geological and geophysical studies for delineation of chromite deposits: a case study from Tangarparha, Orissa, India”, *Geophysics*, Vol. 76, Pp. B173–B185, 2011.

[5] A.K. Chaturvedi, C. Lotter, S. Tripathi, A.K. Maurya, I. Patra, and P.S. Parihar, “Integrated application of heliborne and ground electromagnetic surveys for mapping EM conductor for uranium exploration and its subsurface validation, North Delhi Fold Belt, Rajasthan, India: a case study”, *Geophysics,* Vol. 78, No. 1, Pp. B13–B24, 2013.

[6] I. Patra, A.K. Chaturvedi, P.K. Srivastava, and M.S. Ramayya, “Integrated interpretation of satellite imagery, aeromagnetic, aeroradiometric and ground exploration data sets to delineate favourable target zones for unconformity related uranium mineralisation, Khariar Basin”, *Central India. J. Geol. Soc*. India, Vol. 81, Pp. 299–308, 2013.

[7] D.W. David, P. Kwasi, M.N. Reginald, B. Benjamin, M. Aboagye, K.D. Sylvester, and A. Thomas,“Geophysical Interpretation of Possible Gold Mineralization Zones in Kyerano, South-Western Ghana Using Aeromagnetic and Radiometric Datasets”, *Journal of Geoscience and Environment Protection*, Vol. 3, Pp. 67-82, 2015.

[8] J.O. Ohioma, F.O. Ezomo, and A. Akinsunmade, “Delineation of Hydrothermally Altered Zones that Favour Gold Mineralisation in Isanlu Area, Nigeria Using Aeroradiometric,” *Data International Annals of Science* ISSN: 2456-7132 Volume 2, Issue 1, pp. 20-27, 2017.

[9] J.F. Truswell, and R.N. Cope, “The geology of parts of Niger and Zaria Provinces, Northern Nigeria”, *Geol Survey Nigeria Bull.,* Vol. 29, Pp. 1-104, 1963.

[10] M.A. Rahaman, “Recent advances in the study of the basement complex of Nigeria. In: Geological Survey of Nigeria(ed)”, *Precambrian Geol Nigeria*, Pp. 11-43, 1988.

[11] A. Adediji, and L.T. Ajibade, “The change detection of major dams in Osun State, Nigeria using remote sensing (RS) and GIS techniques”, *Journal of Geography and Regional Planning,* Vol. 1, No. 6, Pp. 110, 2008.

[12] M.N. Nabighian, “The analytical signal of two-dimensional magnetic bodies with polygonal cross –section: Its properties and use for automated anomaly interpretation: Geophysics, Vol. 37, Pp. 507-517, 1972.

[13] W.R. Roest, and M. Pilkington, “Identifying remanent magnetisation effects in magnetic data”, Geophysics, Vol. 58, No. 5, Pp. 653-659, 1993.

[14] D.B. Hoover and H.A. Pierce, “Annotated Bibliography of Gamma-Ray Methods Applied to Gold Exploration”, *U.S.G.S.Open*-File Report, Vol. 90, Pp. 203,23, 1990.

[15] B.L. Dickson and K.M. Scott, “Interpretation of Aerial Gamma-Ray Surveys-Adding the Geochemical Factors, “Journal of Australian Geology and Geophysics, Vol. 17, Pp. 187-200, 1997.

[16] R.J. Griffis, K. Barning, F.L. Ageno, and F.K. Akosah, Gold deposits of Ghana. Minerals Commission Report, 2002.

[17] A.B. Reid, J.M. Allsop, H. Granser, A.T. Millett, and I.W. Somerton, “Magnetic interpretation in three dimensions using Euler deconvolution”, *Geophysics*., Vol. 55, No. 1, Pp. 80-91, 1990.